

In-Situ SEM Observation and DIC Strain Analysis for Deformation and Cracking of Hot-Dip ZnMgAl Alloy Coating

Naoki Takata[†], Hiroki Yokoi, Dasom Kim, Asuka Suzuki, and Makoto Kobashi

Department of Materials Process Engineering, Nagoya University, Nagoya, Aichi, 464-8603, Japan

(Received January 12, 2024; Revised March 23, 2024; Accepted March 24, 2024)

An attempt was made to apply digital image correlation (DIC) strain analysis to in-situ scanning electron microscopy (SEM) observations of bending deformation to quantify local strain distribution inside a ZnMgAl-alloy coating in deformation. Interstitial-free steel sheets were hot-dipped in a Zn-3Mg-6Al (mass%) alloy melt at 400 °C for 2 s. The specimens were deformed using a miniature-sized 4-point bending test machine inside the SEM chamber. The observed in situ SEM images were used for DIC strain analysis. The hot-dip ZnMgAl-alloy coating exhibited a solidification microstructure composed of a three-phase eutectic of fine Al (fcc), Zn (hcp), and Zn₂Mg phases surrounding the primary solidified Al phases. The relatively coarsened Zn₂Mg phases were locally observed inside the ZnMgAl-alloy coating. The DIC strain analysis revealed that the strain was localized in the primary solidified Al phases and fine eutectic microstructure around the Zn₂Mg phase. The results indicated high deformability of the multi-phase microstructure of the ZnMgAl-alloy coating.

Keywords: Hot-dip galvanized steel, Bending test, In-situ observation, Digital image correlation, Local strain

1. Introduction

Hot-dip zinc (Zn) and its alloy coating on steels (galvanized steels) are extensively produced for architectural and automobile applications due to their low cost and sufficient corrosion resistance under atmospheric environments [1,2]. Zn–Mg–Al ternary alloy coatings (ZnMgAl alloy coating) exhibit superior corrosion resistance [3]. The associated hot-dip galvanizing technologies are being applied to building steel parts. One of the significant issues in the application of the hot-dip ZnMgAl alloy galvanizing process to steel parts is the sufficient adhesiveness of the Zn alloy coating layer on the steel parts. It is generally known that the Al-rich Al–Fe intermetallic phase layer consisting of q-Al₁₃Fe₄ and h-Al₅Fe₂ phases [3] is often formed at the interface between the ZnMgAl alloy coating and the steel parts [4-8]. Unfortunately, these Al-rich Al–Fe intermetallic phases are brittle properties [9], likely due to the difficulty of slip deformation at ambient temperature, whereby it is required to control the formation of the Al–Fe intermetallic phases in the ZnMgAl alloy coating on steel parts. Thus,

it is required to understand the interfacial reaction between steel parts and ZnMgAl alloy melt (with a ternary composition of Zn–3%Mg–6%Al) during the hot-dip galvanizing process. We have investigated on the formation sequence of Al–Fe intermetallic phases and its associated growth during the hot-dip galvanizing process for the ZnMgAl alloy coating in conjunction with the calculated Zn–Al–Mg–Fe quaternary phase diagram [10].

The hot-dip galvanizing process produces the solidification microstructures in the Zn alloy coating formed on the steel sheet/strip. It is generally known that the primary solidified Al(fcc) phase and fine three-phase eutectic microstructures composed of Al(fcc), Zn(hcp), and Zn₂Mg phases are often formed in the hot-dip ZnMgAl-alloy galvanized coatings [10,11]. The multi-phase solidification microstructure might exhibit inhomogeneous deformation, which is closely associated with the deformability of the ZnMgAl-alloy coatings in the plastic-forming process. In particular, the Zn₂Mg intermetallic phase exhibits brittle properties as well as the Al-rich Al–Fe intermetallic phases, whereby it is necessary to understand the role of the Zn₂Mg intermetallic phase in the deformation of the ZnMgAl-alloy coating on the steel sheets in the plastic-forming process.

[†]Corresponding author: takata.naoki@material.nagoya-u.ac.jp

To better understand the effect of the multi-phase solidification microstructure on the deformation of hot-dip ZnMgAl-alloy coating in terms of the Zn₂Mg intermetallic phase, in this study, an attempt was made to use the in-situ SEM observation combined with the digital image correlation (DIC) strain analysis for the solidification microstructure of the Zn-3%Mg-6%Al alloy coating on the steel sheet in bending test.

2. Experimental

In the present study, interstitial-free (IF) steel sheets were used as a model of pure iron with a ferrite (α-Fe) single-phase microstructure. The steel sheet was hot-rolled and then cold-rolled to about 1.5 mm in thickness. Hot-dipping experiments were carried out using a hot-dip process simulator [12,13]. Before the hot-dipping experiment, the steel sheets were mechanically polished and then finished with buffing compounds. The alloy sheets with an approximate dimension of 210 mm × 105 mm × 1.2 mm were heated to 800 °C for 60 s, and then cooled down to a bath temperature of 400 °C under N₂-50 vol.% H₂ atmosphere. After that, these sheets were hot-dipped in a molten Zn-3Mg-6Al (mass%) alloy bath at 400 °C for 2 s, followed by rapid cooling by using the

gas wiping system. The microstructures of the prepared samples were observed by scanning electron microscope (SEM) operating at 20 kV. The observed sample surfaces were mechanically polished and then finished using colloidal silica. The low-magnification SEM images were used to measure the thickness of the IF steel sheets. For high-magnification SEM observation, the sample surface was ion-polished with a cross-section polisher operated at 6 kV.

The appearance of the miniature-sized 4-point bending test machine (TSL Solutions Inc. BS-500) and the specimen geometry [14] are presented in Fig. 1a and 1b. The bending test machine loaded with an experimental plate-shaped specimen was placed inside the vacuum chamber of the SEM instrument (JEOL JSM-6610) for in-situ observation of the ion-polished surfaces, as presented in Fig. 1c. Note that the specimen surface for SEM observations was ion-polished with a cross-section polisher operated at 6 V. The macroscopic strain (ϵ_m) applied to the surface of the bent specimen was calculated by the following equation:

$$\epsilon_m = t / 2R \quad (1)$$

where t is the specimen thickness (approximately 1.5 mm)

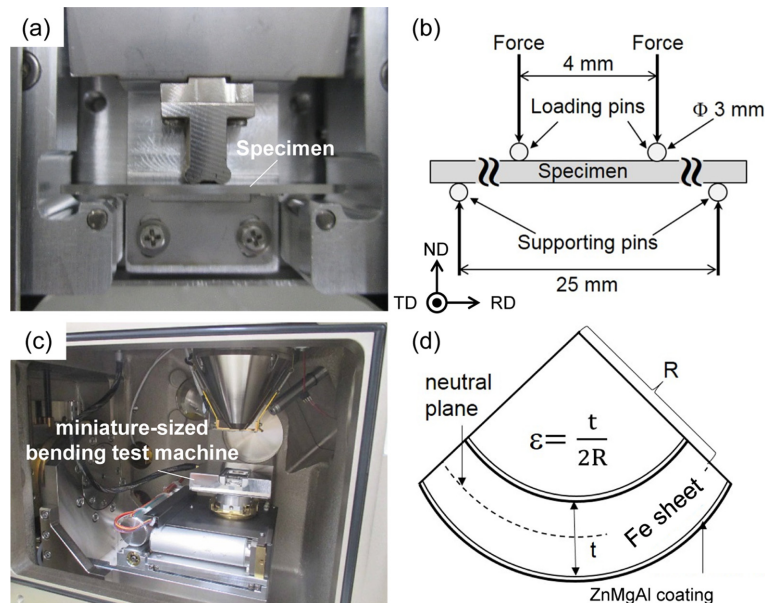


Fig. 1. Schematic illustrations showing (a) a specimen mounted in a miniature-sized bending test machine, (b) a geometry of used specimens associated with fulcrum points for a four-point bending test applied [14], (c) a designed miniature-sized bending test machine fitting into an SEM chamber for in-situ observation, and (d) a bent specimen geometry

and R is the radius of curvature measured using the in-situ observed low-magnification SEM images, as schematically shown in Fig. 1d. The local strain distribution in the ZnMgAl-alloy coating of the bent specimens was quantified by digital image correlation (DIC) analysis [15] using the in-situ observed SEM images at different states of deformation. In the present study, DIC analysis software (Correlated Solutions Inc. VIC-2D) was performed using high-magnification SEM images at a subset size of approximately 5 mm for the captured SEM images.

3. Results and Discussion

3.1 In-situ SEM observation in bending test

Fig. 2 presents a representative load-displacement curve of the hot-dip ZnMgAl-alloy galvanized steel specimens in the bending tests. Stress drops are often observed in the flow curve of bending tests conducted in the SEM chamber when the bending must be interrupted to allow careful SEM observations of microstructure in the

ZnMgAl-alloy coating. These stress drops correspond to the stress relaxations in the specimen during the interrupting bending test for in-situ SEM observations. Nevertheless, the flow curves exhibit a yielding and subsequent strain hardening and agree well with the curve from uninterrupted bending tests conducted outside the

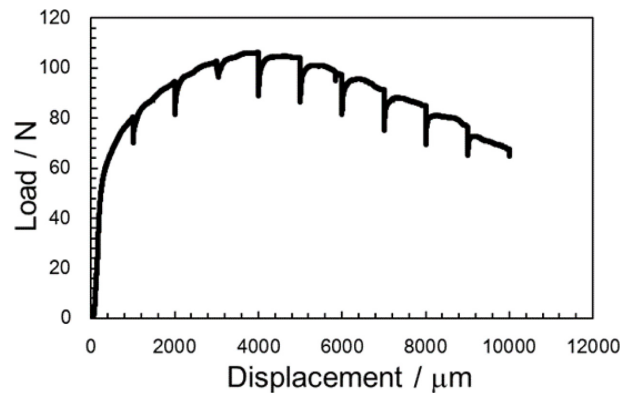


Fig. 2. Representative load-displacement curve of the hot-dip ZnMgAl-alloy coated IF steel sheet measured by the miniature-sized bending test machine

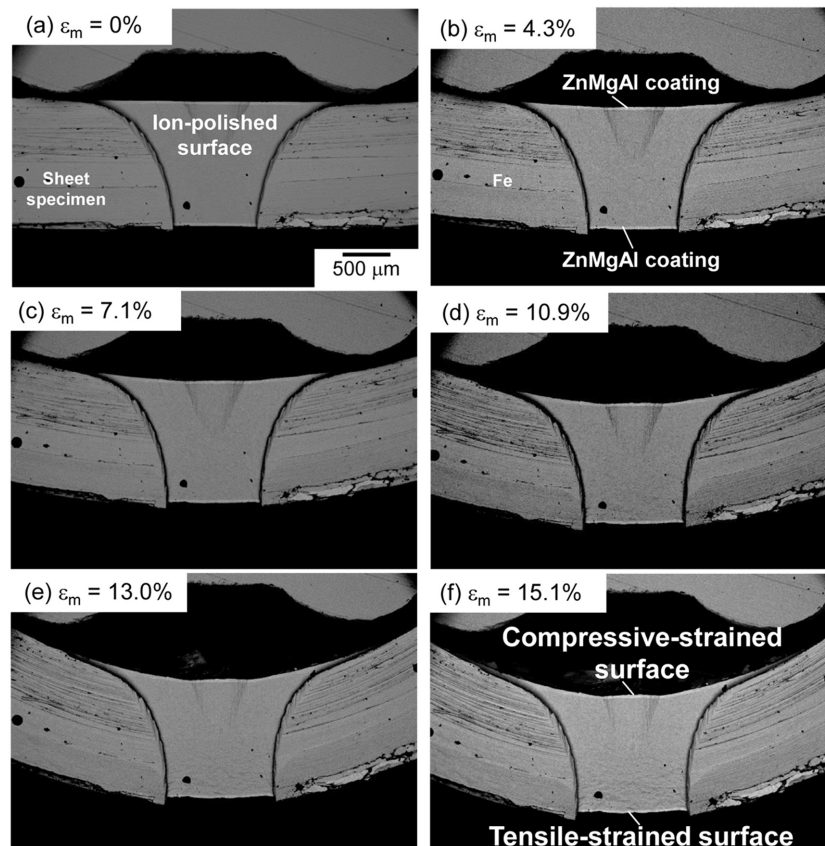


Fig. 3. Low-magnification SEM images showing the bent specimens at different macroscopic strains, ϵ_m (measured by curvature of the specimen surface)

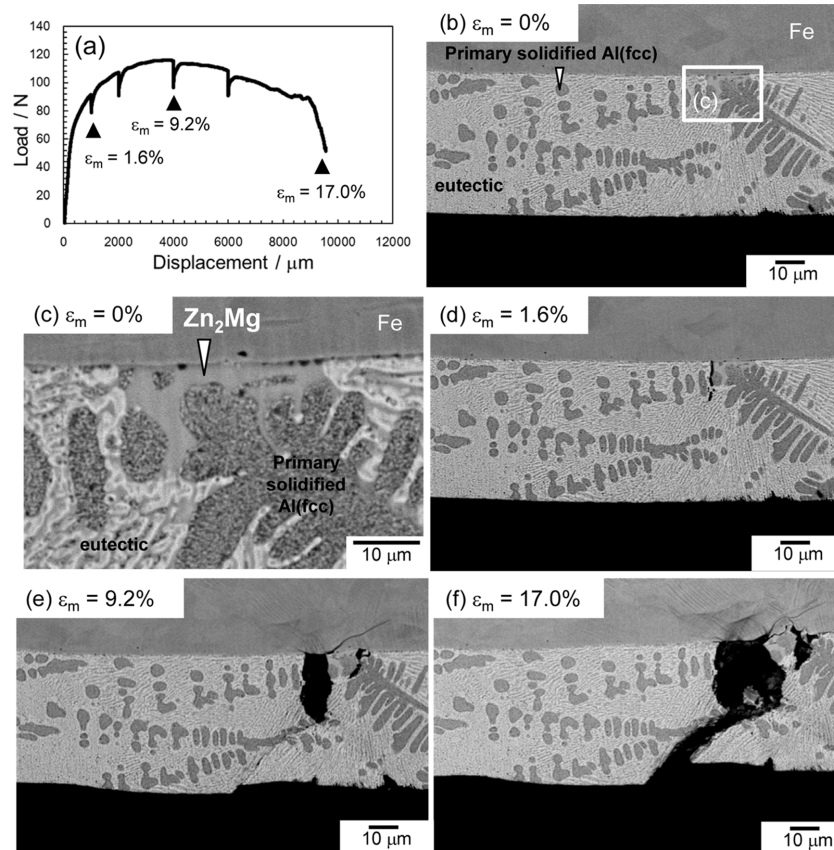


Fig. 4. (a) Load-displacement curve and (b-f) corresponding in-situ observed SEM backscattered-electron images showing the initiated and propagated cracks in the ZnMgAl coating layer on the tensile-strained surface of the sheet specimen. Macroscopic strains (ϵ_m) were calculated to be approximately (d) 1.6 %, (e) 9.2 %, and (f) 17.0 %

SEM chamber.

Low-magnification in-situ SEM images obtained during the bending test are displayed in Fig. 3. The specimen was uniformly deformed with an increasing punch stroke (displacement). For the specimens deformed at different displacements, the radius (R) of curvature was experimentally measured using the in-situ observed images (Fig. 3). Note that the observed V-shaped area on the cross-section of the specimen corresponds to the observed ion-polished surface. The measured R values can be used to calculate the macroscopic strains (ϵ_m) of the specimen following equation (1) (as schematically illustrated in Fig. 1d). The calculated ϵ_m approximately ranged from 4 % to 15 % for different displacements, as labeled in Fig. 3.

Fig. 4 presents a load-displacement curve of the specimen measured by the bending test and corresponding in-situ observed backscattered electron images (BEIs) showing the microstructure of the hot-dip ZnMgAl-alloy

coating on the tensile-strained surface of the bent specimen. A number of dendritic Al(fcc) phases surrounded by fine eutectic microstructures composed of Al(fcc), Zn(hcp), and Zn₂Mg phases were observed in the present ZnMgAl-alloy coating formed on the steel sheet (Fig. 4b). Relatively coarsened Zn-rich intermetallic phases (corresponding to the Zn₂Mg phase in the present alloy system) were locally found inside the coating (Fig. 4b, c). An identified area showing the relatively coarsened Zn₂Mg phase in the ZnMgAl-alloy coating was in-situ observed in the bending test. The observed images obviously show that a vertical crack was initiated inside the brittle Zn₂Mg intermetallic phase at an early stage of deformation under a macroscopic strain of $\epsilon_m = 1.6\%$ (Fig. 4d). This vertical crack opened and propagated inside the fine eutectic microstructure under the tensile deformation (Fig. 4e). The crack tip appeared to contact the dendritic Al(fcc) phase (presumably exhibiting higher deformability), suggesting the suppressed crack propagation.

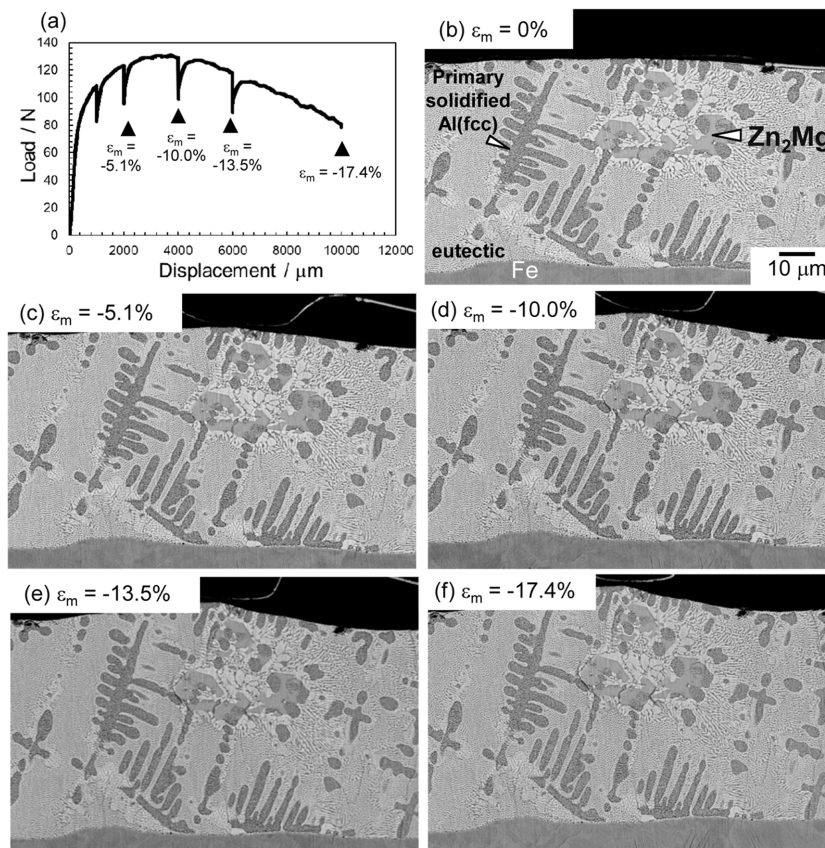


Fig. 5. (a) Load-displacement curve and (b-f) corresponding in-situ observed SEM backscattered-electron images showing the microstructure of the ZnMgAl coating layer on the compressive-strained surface of the sheet specimen; Macroscopic strains (ϵ_m) were calculated to be approximately (c) -5.1 %, (d) -10.0 %, (e) -13.5 %, and (f) -17.4 %

However, the initiated crack penetrated the coating layer at a higher tensile strain of $\epsilon_m = 17.0\%$ (Fig. 4f). In addition, note that extensive slip traces were observed in the steel sheet, in particular around the cracks (Fig. 4e, f), which is indicative of the occurrence of slip deformation localized around the initiated cracks.

Fig. 5 displays a load-displacement curve of the specimen measured by the bending test and corresponding in-situ observed BEIs showing the microstructure of the hot-dip ZnMgAl-alloy coating on the compressive-strained surface of the bent specimen. Many dendritic Al(fcc) phases surrounded by the fine eutectic microstructure were observed as well, whereas relatively coarsened Zn_2Mg phases with granular morphologies were locally observed (Fig. 5b). A selected area showing the granular Zn_2Mg phase was in-situ observed in the ZnMgAl-alloy coating under compression. The observed images clearly represent that no crack was initiated around/inside the granular Zn_2Mg phase (Fig. 5c-f), even

at a high compressive strain of $\epsilon_m = -17.4\%$ (Fig. 5f). The result indicates the coarsened Zn_2Mg phase have a slight effect on cracking in the hot-dip ZnMgAl-alloy coating under compression.

3.2 Local strain distribution analyses for in-situ observed SEM images

To understand the inhomogeneous deformation associated with the relatively coarsened Zn_2Mg phase in the ZnMgAl-alloy coating under tension or compression, the local strain distribution was quantified by DIC analysis of the in-situ observed SEM images in the tensile-strained and compressive-strained surface regions (as presented in Fig 4 and Fig. 5). The results from the DIC analysis are summarized in Fig. 6 and Fig. 7. The visualized strain maps of ϵ_{xx} are presented in these figures, with the horizontal and vertical directions defined as x and y directions, respectively. The crack initiated at a low macroscopic strain of $\epsilon_m = 1.6\%$ under tension (Fig. 4d),

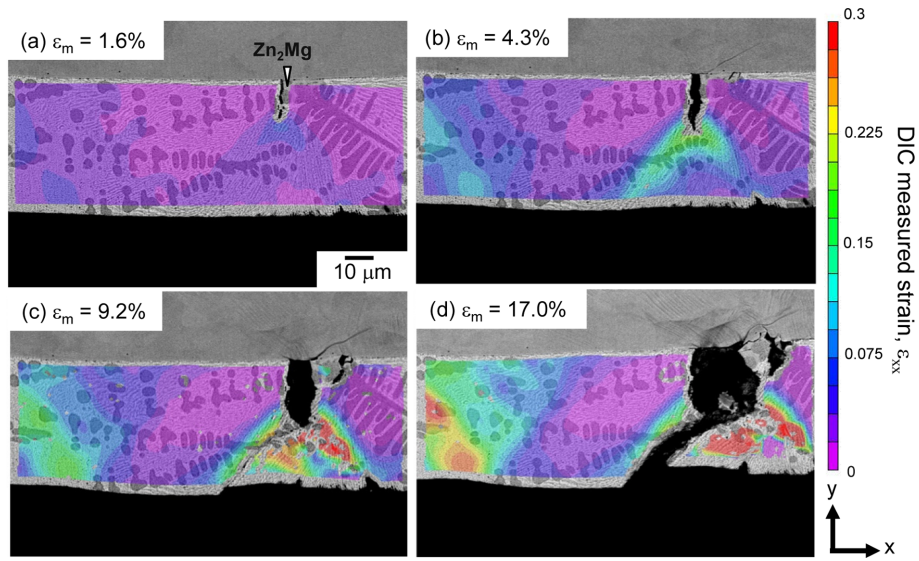


Fig. 6. DIC analyzed strain distribution maps (ϵ_{xx}) for in-situ observed SEM backscattered-electron images showing the initiated and propagated cracks in the ZnMgAl coating layer on the tensile-strained surface of the sheet specimen

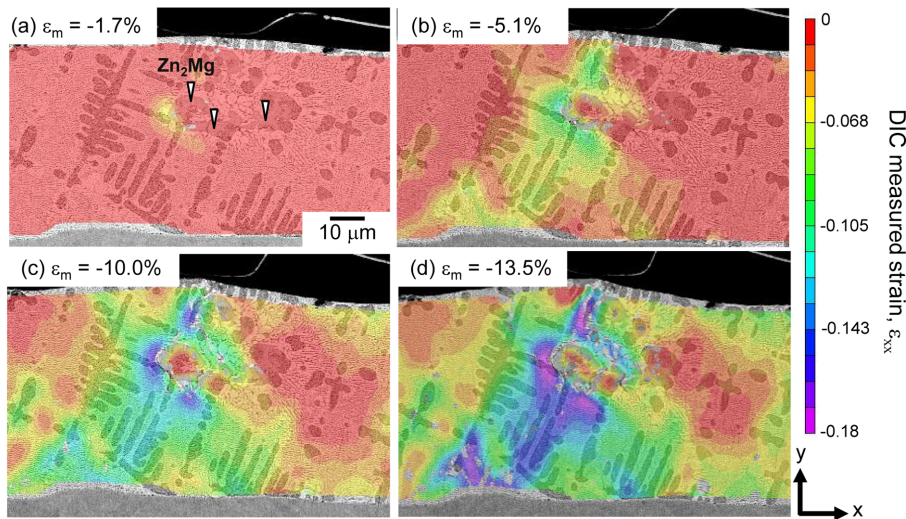


Fig. 7. DIC analyzed strain distribution maps (ϵ_{xx}) for the in-situ observed SEM backscattered-electron images showing the microstructure of the ZnMgAl coating layer on the compressive-strained surface of the sheet specimen

and a significant strain localization was not detected around the crack (Fig. 6a), indicating the brittle fracture occurring in the Zn_2Mg phase. However, the strain localization appeared more pronounced around the crack tip at a higher macroscopic strain (Fig. 6b, c). The occurrence of plastic deformation in the dendritic Al phases and fine eutectic microstructures would reduce the stress/strain localization (for crack propagation) around the tip of the propagated crack. Under compression (Fig. 7), the strain localization was scarcely observed inside the relatively coarsened Zn_2Mg phase, whereas the compressive strain

(negative value of ϵ_{xx}) was localized around the Zn_2Mg phase (Fig. 7a). The tendency appeared more significant by applying higher macroscopic strain (Fig. 7b-d). These results demonstrated high deformability of the dendritic Al phases and fine eutectic microstructures in the ZnMgAl-alloy coating under tension and compression. The elimination of the locally formed Zn_2Mg phase (with brittle properties) in the hot-dip galvanizing process could be, therefore, necessary to prevent the local cracking occurring in the ZnMgAl-alloy coating in the plastic-forming process (in particular, stretch forming process).

4. Summary

The present paper proposed a novel experimental approach of the in-situ SEM observation of the 4-point bending test combined with the digital image correlation (DIC) strain analysis for quantification of the local strain distribution inside the ZnMgAl-alloy coating in deformation. The present ZnMgAl-alloy coating exhibited the solidification microstructure composed of a three-phase eutectic of fine Al (fcc), Zn (hcp), and Zn₂Mg phases surrounding the primary solidified Al phases. The relatively coarsened Zn₂Mg phases were locally observed inside the ZnMgAl-alloy coating. After the bending test, no crack was found on the compressive-strained surface of the ZnMgAl-alloy coated steel specimen, while vertical cracks were found on the tensile-strained surface. The in-situ SEM observations revealed that cracks were initiated inside the relatively coarsened Zn₂Mg phase in the ZnMgAl alloy coating and then penetrated the inside of the coating under tension. The DIC analyses revealed that the strain was localized in the primary solidified Al phases and fine eutectic microstructure around the Zn₂Mg phase, indicating high deformability of the multi-phase microstructure of the ZnMgAl-alloy coating under tension and compression. The proposed experimental approach would be effective in understanding the deformation of the galvanized coating on steel sheets [16].

References

1. A. R. Marder, The Metallurgy of Zinc-Coated Steel, *Progress in Materials Science*, **45**, 191 (2000). Doi: [http://dx.doi.org/10.1016/S0079-6425\(98\)00006-1](http://dx.doi.org/10.1016/S0079-6425(98)00006-1)
2. D. Mizuno, Automotive Corrosion and Accelerated Corrosion Tests for Zinc Coated Steels, *ISIJ International*, **58**, 1562 (2018). Doi: <https://doi.org/10.2355/isijinternational.ISIJINT-2018-159>
3. R.W. Richards, R.D. Jones, P.D. Clements, and H. Clarke, Metallurgy of continuous hot dip aluminizing, *International Materials Reviews*, **39**, 191 (1994). Doi: <https://doi.org/10.1179/imr.1994.39.5.191>
4. K. Honda, K. Ushioda, and W. Yamada, Influence of Si Addition to the Coating Bath on the Growth of the Al-Fe Alloy Layer in Hot-dip Zn-Al-Mg Alloy-coated Steel Sheets, *ISIJ International*, **51**, 1895 (2011). Doi: <https://doi.org/10.2355/isijinternational.51.1895>
5. Y. Chen, Y. Liu, H. Tu, C. Wu, X. Su, and J. Wang, Effect of Ti on the growth of the Fe-Al layer in a hot dipped Zn-6Al-3Mg coating, *Surface and Coatings Technology*, **275**, 90 (2015). Doi: <https://doi.org/10.1016/j.surfcoat.2015.05.034>
6. K. Li, Y. Liu, H. Tu, X. Su, and J. Wang, Effect of Si on the growth of Fe-Al intermetallic layer in Zn-11%Al-3%Mg coating, *Surface and Coatings Technology*, **306**, 390 (2016). Doi: <https://doi.org/10.1016/j.surfcoat.2016.05.033>
7. J.-K. Chang and C.-S. Lin, Microstructural Evolution of 11Al-3Mg-Zn Ternary Alloy-Coated Steels During Austenitization Heat Treatment, *Metallurgical and Materials Transactions A*, **48**, 3734 (2017). Doi: <https://doi.org/10.1007/s11661-017-4126-6>
8. Y. Xie, A. Du, X. Zhao, R. Ma, Y. Fa, and X. Cao, Effect of Mg on Fe-Al interface structure of hot-dip galvanized Zn-Al-Mg alloy coatings, *Surface and Coatings Technology*, **337**, 313 (2018). Doi: <https://doi.org/10.1016/j.surfcoat.2018.01.038>
9. T. Tsukahara, N. Takata, S. Kobayashi, and M. Takeyama, Mechanical Properties of Fe₂Al₃ and FeAl₃ Intermetallic Phases at Ambient Temperature, *Tetsu-to-Hagané*, **102**, 89 (2016). Doi: <https://doi.org/10.2355/tetsutohagane.TETSU-2015-063>
10. H. Yokoi, N. Takata, A. Suzuki, and M. Kobashi, Formation sequence of Fe-Al intermetallic phases at interface between solid Fe and liquid Zn-6Al-3Mg alloy, *Intermetallics*, **109**, 74 (2019). Doi: <https://doi.org/10.1016/j.intermet.2019.03.011>
11. S. Tanaka, K. Honda, A. Takahashi, Y. Morimoto, M. Kurosaki, H. Shindo, K. Nishimura, and M. Sugiyama, Proc. 5th Int. Conf. on Zinc and Zinc Alloy Coated Steel (Galvatech '01), pp. 153 – 160, Brussels, Belgium (2001).
12. A. Nishimoto, J. Inagaki, and K. Nakaoka, Influence of Alloying Elements in Hot Dip Galvanized High Tensile Strength Sheet Steels on the Adhesion and Iron-zinc Alloying Rate, *Tetsu-to-Hagané*, **68**, 1404 (1982). Doi: https://doi.org/10.2355/tetsutohagane1955.68.9_1404
13. L. Chen, R. Fourmentin, and J. R. McDermid, Morphology and Kinetics of Interfacial Layer Formation during Continuous Hot-Dip Galvanizing and Galvannealing, *Metallurgical and Materials Transactions A*, **39**, 2128 (2008). Doi: <https://doi.org/10.1007/s11661-008-9552-z>
14. H. Li, N. Takata, M. Kobashi, and A. Serizawa, In Situ Scanning Electron Microscopy Observation of Crack Initiation and Propagation in Hydroxide Films Formed by Steam Coating on Aluminum-Alloy Sheets, *Materials*, **13**,

- 1238 (2020). Doi: <https://doi.org/10.3390/ma13051238>
15. B. Pan, Recent Progress in Digital Image Correlation, *Experimental Mechanics*, **51**, 1223 (2011). Doi: <https://doi.org/10.1007/s11340-010-9418-3>
16. D. Kim, N. Takata, H. Yokoi, A. Suzuki, and M. Kobashi, Microstructural factors controlling crack resistance of Zn-Al-Mg alloy coatings prepared via hot-dip galvanizing process: Combined approach of in-situ SEM observation with digital image correlation analysis, *Journal of Materials Research and Technology*, **29**, 1535 (2024). Doi: <https://doi.org/10.1016/j.jmrt.2024.01.235>